Electronic Supplementary Material (ESI) for CrystEngComm.

Electronic Supplementary Information

Performance enhancement of self-biased n-ZnO microwire/p-GaN heterojunction ultraviolet photodetector incorporating AgNWs

Yulan Xie, Peng Wan, Mingming Jiang,* Yang Liu, Daning Shi and Caixia Kan*

College of Physics, MIIT Key Laboratory of Aerospace Information Materials and Physics, Key Laboratory for Intelligent Nano Materials and Devices, Nanjing University of Aeronautics and Astronautics, No. 29 Jiangjun Road, Nanjing 211106, China.

**E-mail: mmjiang@nuaa.edu.cn; cxkan@nuaa.edu.cn.*

Supplementary figures

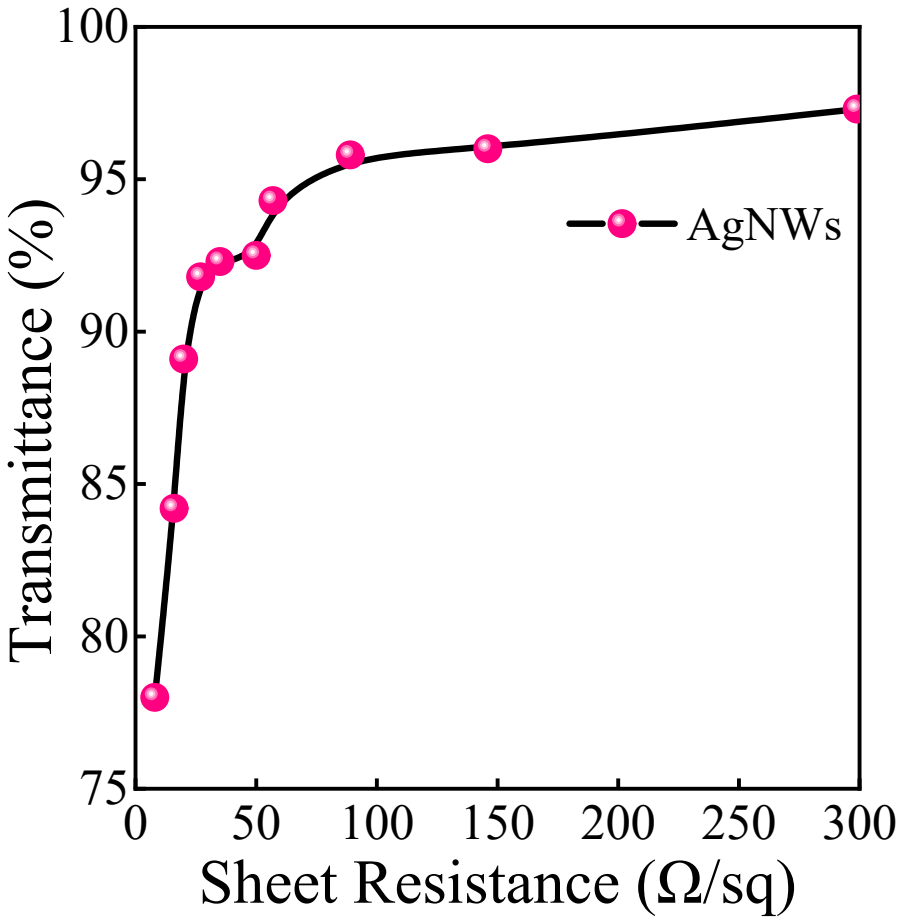

Figure. S1: Plots of optical transmittance (λ = 370 nm) versus sheet resistance for AgNWs films.

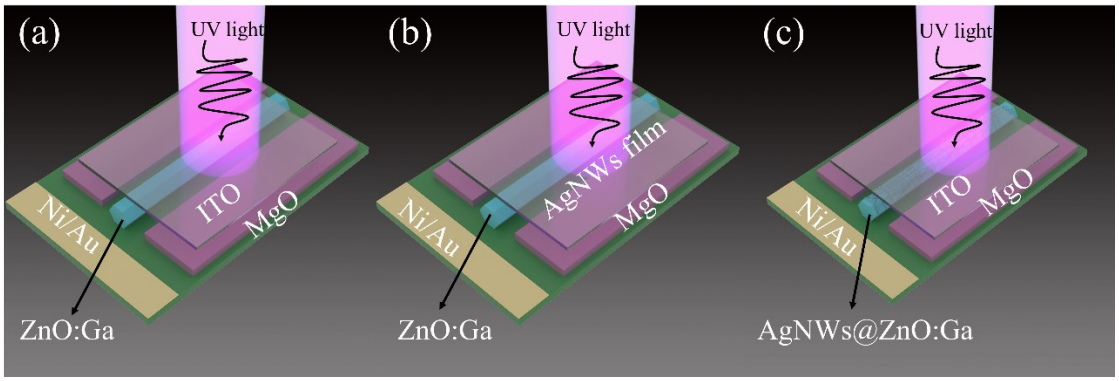

Figure. S2: (a) Schematic architecture of Device-1, which is composed of ZnO:Ga MW, p-type GaN film, and ITO electrode. (b) Schematic architecture of Device-2, which is composed of AgNWs@ZnO:Ga MW, p-type GaN film, and AgNWs transparent electrode. (c) Schematic architecture of Device-3, which is composed of AgNWs@ZnO:Ga MW, p-type GaN film, and ITO electrode.

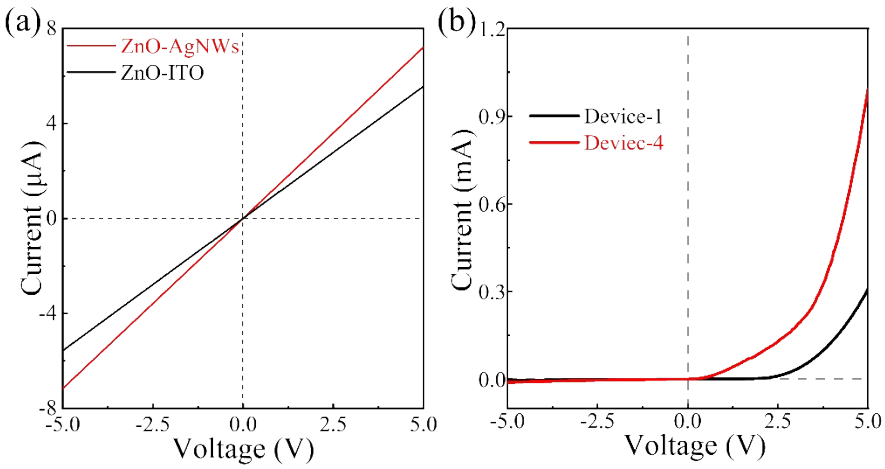

Figure S3: (a) the current-voltage (*I-V*) curves of the ZnO-AgNWs and ZnO-ITO structures. (b) Room-temperature *I-V* curves of Device-1 and Device-4.

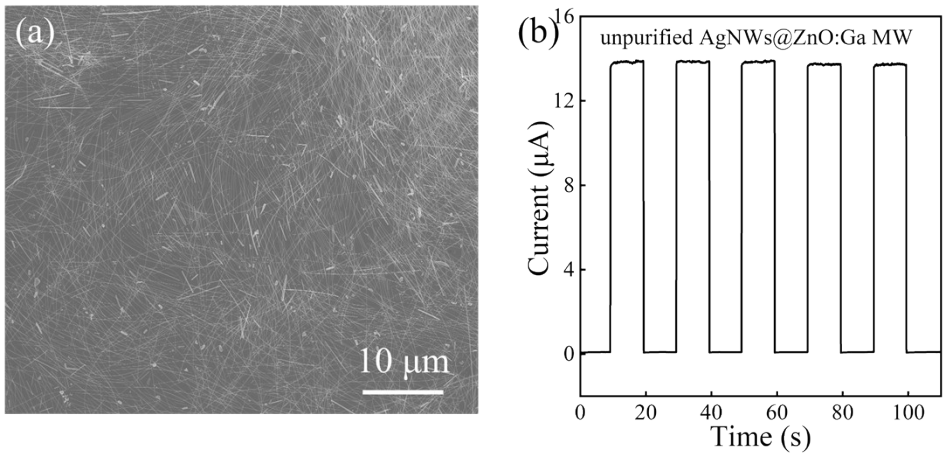

Figure S4: (a) SEM image of AgNWs before purification. (b) *I-T* curve of the fabricated ITO/n-AgNWs@ZnO:Ga MW/p-GaN heterojunction device when operated upon 370 nm illumination in a self-powered mode (the AgNWs hasn't been purified).

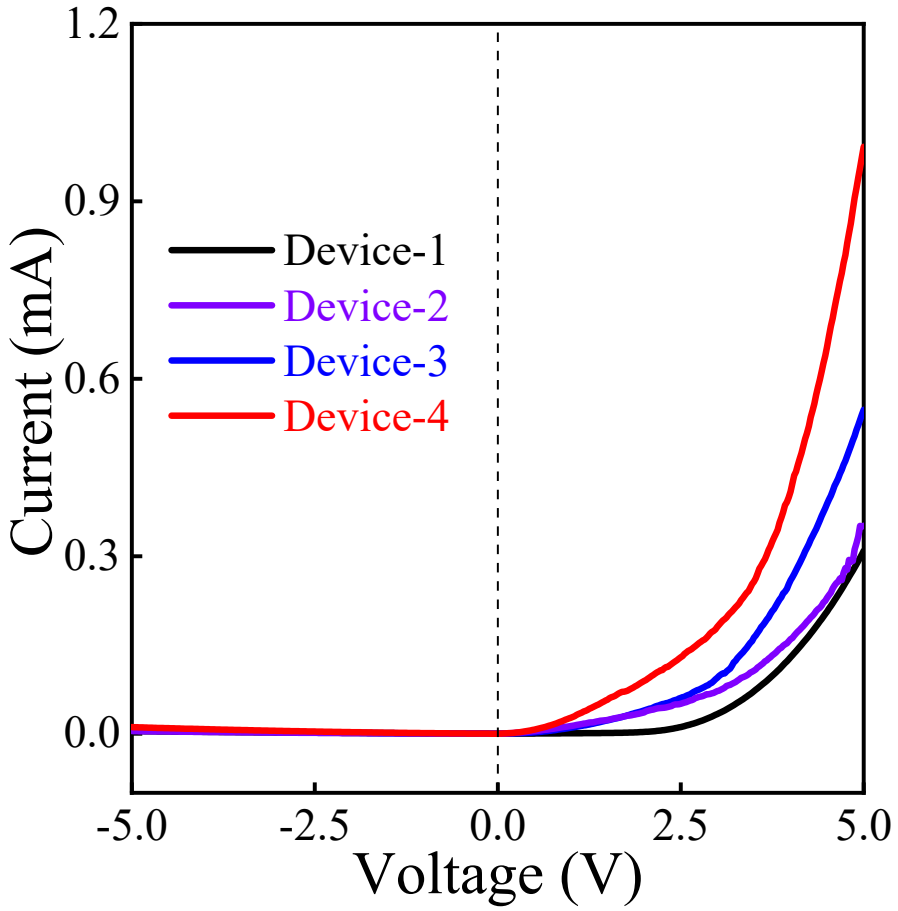

Figure. S5: I-V curves of the Device-1, Device-2, Device-3 and the Device-4 under dark.

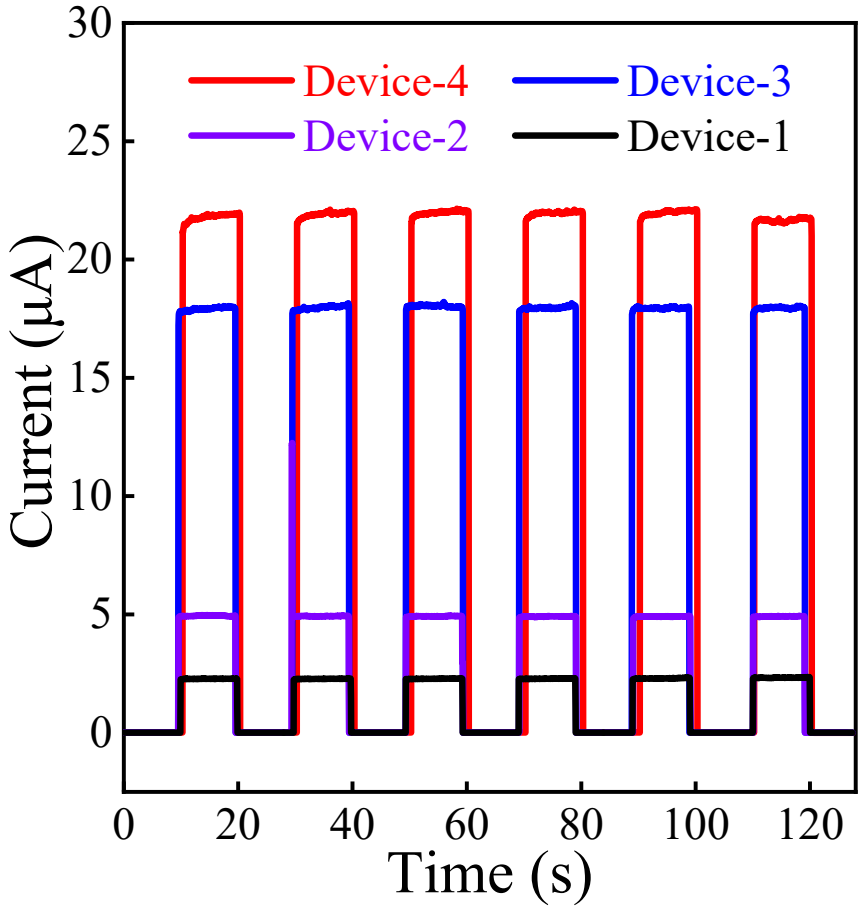

Figure. S6: Time-resolved photocurrent curves of the Device-1, Device-2, Device-3, and Device-4 with the ultraviolet light (370 nm, 0.50 mW/cm^2) on and off at the voltage of 0 V.

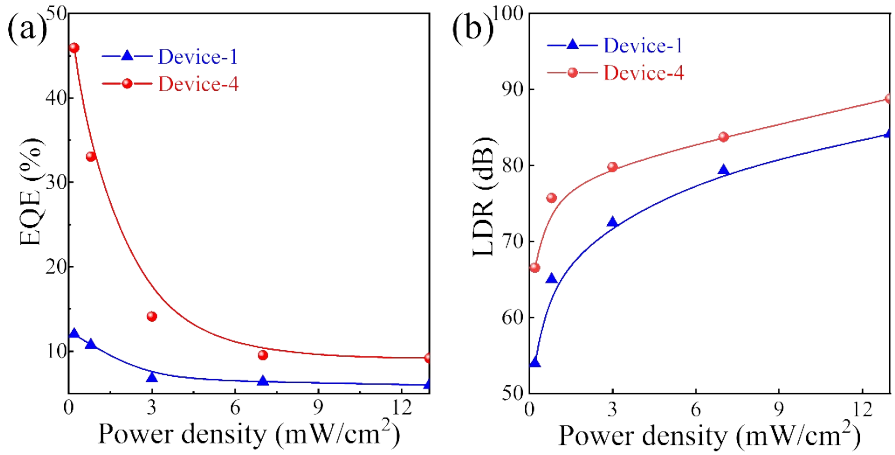

Figure S7: Comparison of the calculated EQE (a), LDR (b) of the fabricated Device-1 and Device-4 under the ultraviolet light of 370 nm with the varied power densities.

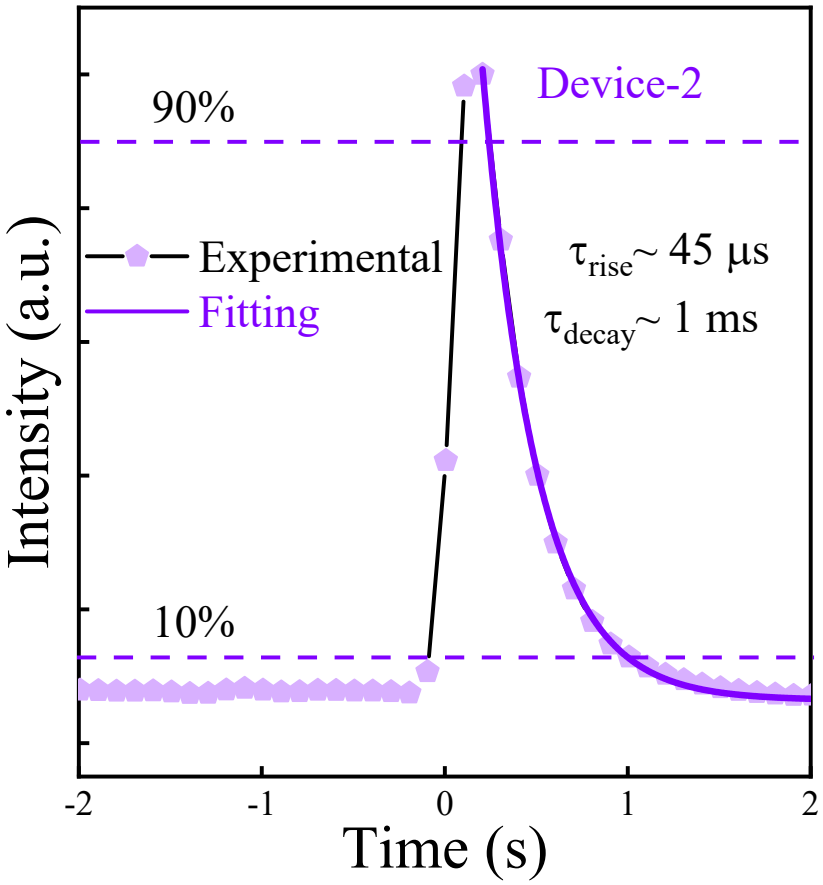

Figure. S8: One-cycle transient time-resolved response of Device-3 under 370 nm pulse laser illumination at zero bias voltage.

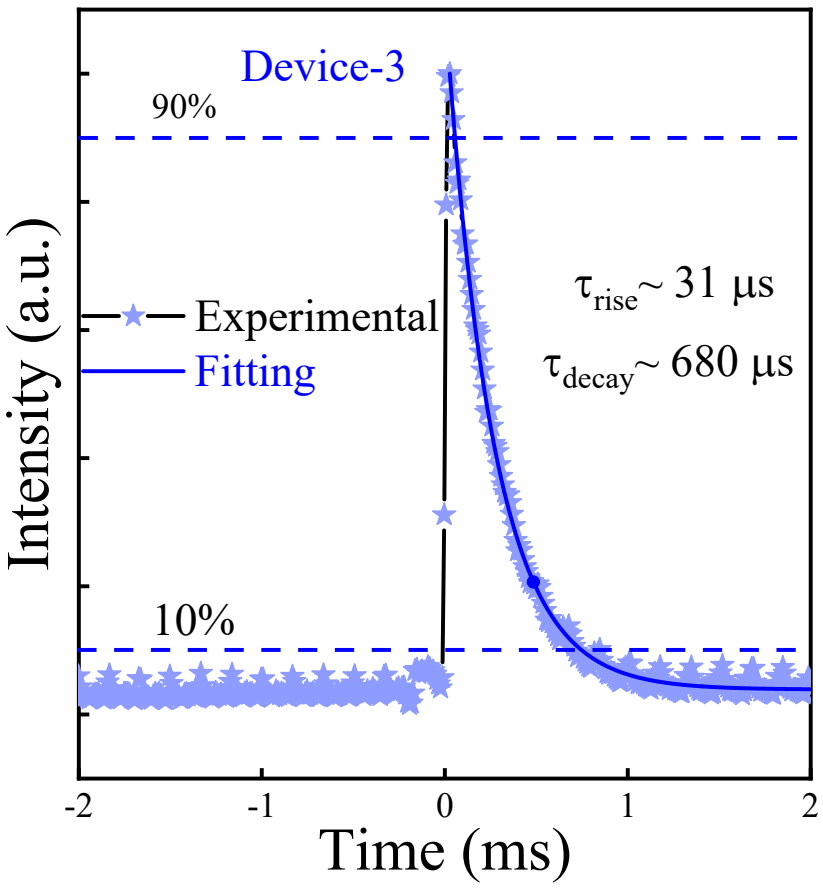

Figure. S9: One-cycle transient time-resolved response of Device-3 under 370 nm pulse laser illumination at zero bias voltage.

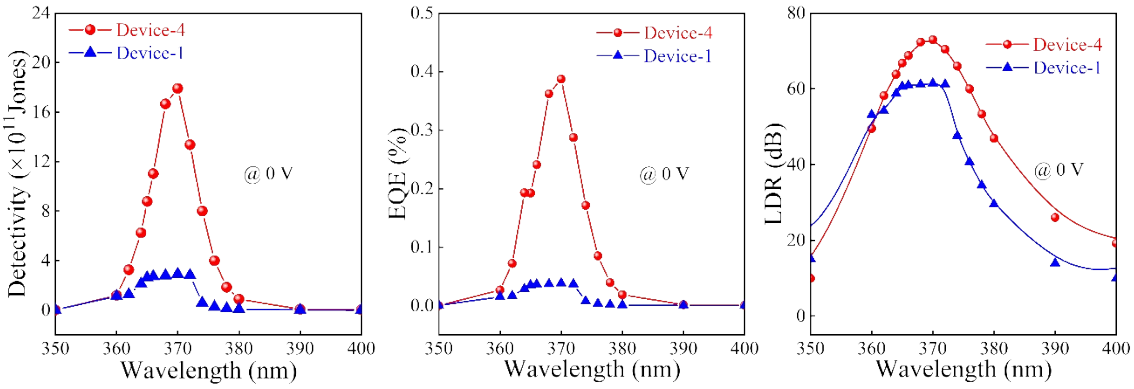

Figure S10: Comparison of the calculated (a) D*, (b) EQE, and (c) LDR of the fabricated heterojunction devices under zero bias with the varied wavelength from 350 nm to 400 nm.

Table-S1: A comparison between the detection performance in Device-1, Device-2, Device-3, Device-4.

Photodetector	Device-1	Device-2	Device-3	Device-4
Current (-5V)	4.37×10^{-6} (A)	4.40×10^{-6} (A)	6.59×10^{-6} (A)	1.11×10^{-5}（A）
Current (5V)	3.09×10^{-4}（A）	3.51×10^{-4}（A）	5.47×10^{-4}（A）	9.92×10^{-4}（A）
Rectification ratio	70.7	79.8	83.0	89.3
Dark current (0V)	2.15×10^{-9} (A)	4.5×10^{-9} (A)	9.56×10^{-9} (A)	1.0×10^{-8} (A)
Photocurrent (0V)	2.27×10^{-6} (A)	4.92×10^{-6} (A)	1.78×10^{-5} (A)	2.15×10^{-5} (A)
I_{ph}/I_d ratio	1135	1225	1935	2200

Table-S2: Device characteristics.

Photodetector	Wavelength (nm)	Responsivity (mA/W)	Detectivity (Jones)	Rise/decay time
Device-1	370	12	3.08×10^{11}	47 μs/1.08 ms
Device-2	370	24.58	4.10×10^{11}	45 μs/1 ms
Device-3	370	88.95	1.02×10^{12}	31/680 μs
Device-4	370	137	2.15×10^{12}	22/339 μs